Quantification of Silane Molecules on Oxidized Silicon: Are there Options for a Traceable and Absolute Determination?

P. M. Dietrich,[1*] C. Streeck,[2] S. Glamsch,[1,4] C. Ehlert,[1,3] A. Lippitz,[1] A. Nutsch,[2] N. Kulak,[4] B. Beckhoff,[2] and W. E. S. Unger[1]

[1] Bundesanstalt für Materialforschung und -prüfung (BAM), Unter den Eichen 87, 12205 Berlin, Germany.

[2] Physikalisch-Technische Bundesanstalt (PTB), Abbestr. 2-12, 10587 Berlin, Germany.

[3] Institut für Chemie, Universität Potsdam, Karl-Liebknecht-Straße 24-25, 14476 Potsdam, Germany.

[4] Freie Universität Berlin, Institut für Chemie und Biochemie, Fabeckstr. 34/36, 14195 Berlin, Germany.

[*]Corresponding author: paul.dietrich@bam.de

Content

1. Methods

NMR spectroscopy and mass spectrometry. ^{1}H NMR spectra were recorded on a Jeol ECX 400 instrument. ESI-MS samples were measured on an Agilent 6210 ESI-TOF, Agilent Technologies, Santa Clara, CA, USA. The solvent flow rate was adjusted to 4 µL/min, the spray voltage set to 4 kV, and drying gas flow rate was set to 15 psi (1 bar). All other parameters were adjusted for a maximum abundance of the relative [M+Na]$^+$. EI-MS samples were measured on a MAT 711, Varian MAT, Bremen. Electron Energy for EI was set to 80 eV (120 °C).

2. Synthesis of Benzamidosilane 2
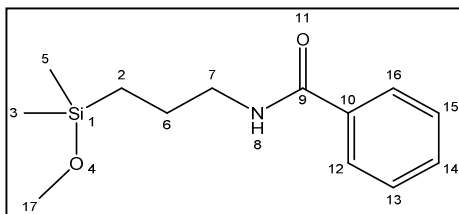
N-(3-(methoxydimethylsilyl)propyl)benzamide (**2**)[1]. To an ice-cooled solution of 0.87 ml (1.0 eq) of **1** in 10 ml dichloromethane, 0.69 ml (1.1 eq) benzoyl chloride and 0.83 ml (1.1 eq) triethylamine were added under stirring. After stirring at room temperature for 2 h the yellow solution was poured into ice-cooled water and extracted three times with 20 ml dichloromethane each. Then the organic phase was dried over sodium sulfate for 30 min, filtrated and the solvent was removed under reduced pressure giving 0.99 g (67%) of **2** as yellow oil. The product was stored under Ar atmosphere till further use.

^{1}H-NMR (400 MHz, CDCl$_3$): δ= 0.11 (s, 6H, H^{3,5}), 0.65 (t, J= 8 Hz, 2H, H^2), 1.66 (quint, J= 8 Hz, 2H, H^6), 3.41-3.45 (m, 5H, H^{7,17}), 6.47 (s, 1H, H^8), 7.40-7.76 ppm (m, 5H, H$^{12-16}$). EI-MS: $m/z = 236.3$ (calc. for C$_{12}$H$_{18}$NO$_2$Si: $m/z = 236.1$) $[M - CH_3]^+$. ESI-MS: $m/z = 274.1222$ (calc. for C$_{12}$H$_{18}$NO$_2$Si: $m/z = 274.1234$) $[M + Na]^+$.
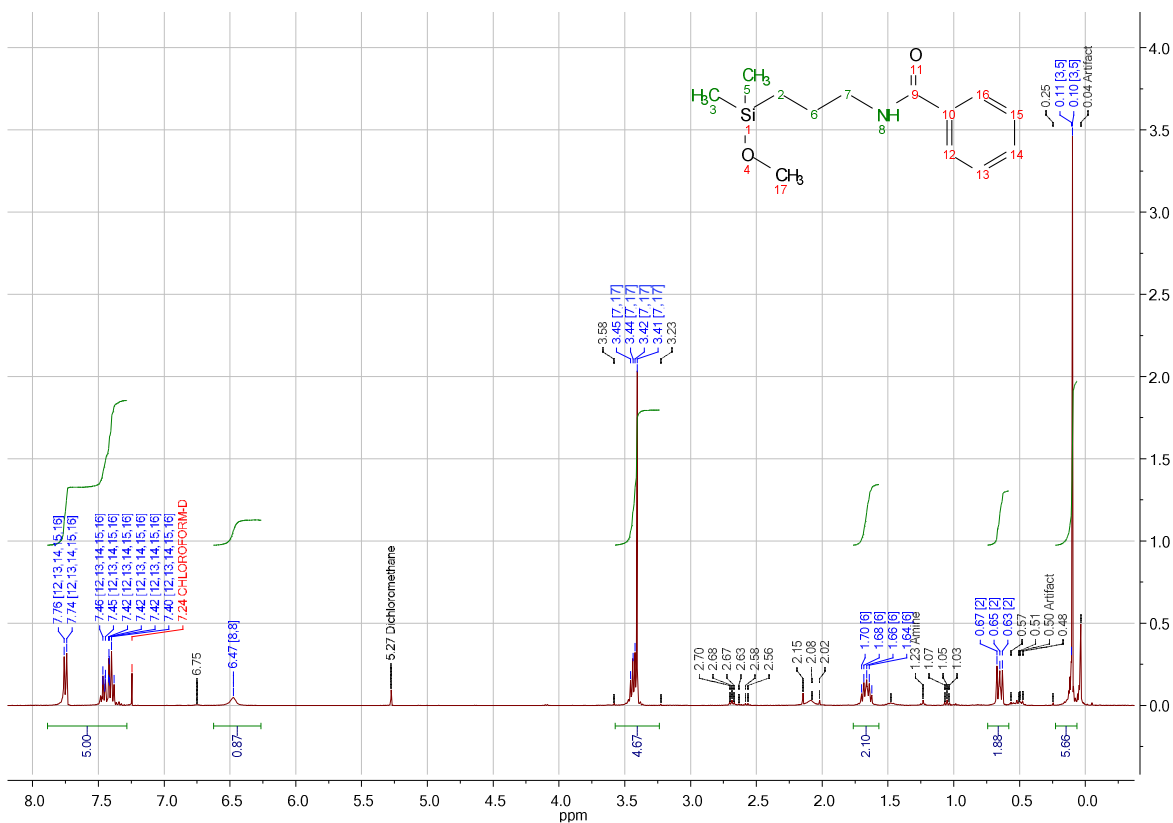
Figure S1. ^{1}H-NMR spectrum of *N*-(3-(methoxydimethylsilyl)propyl)¬benzamide (**2**) in CDCl$_3$ at 400 MHz.
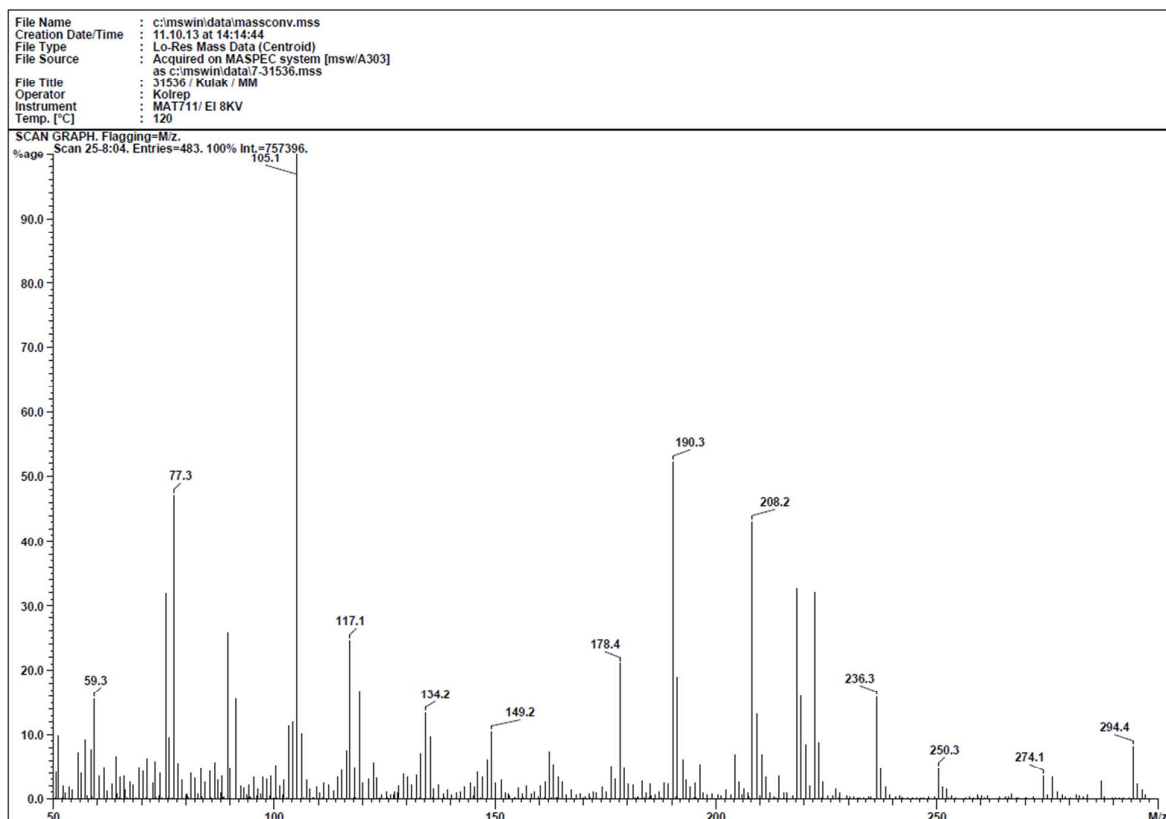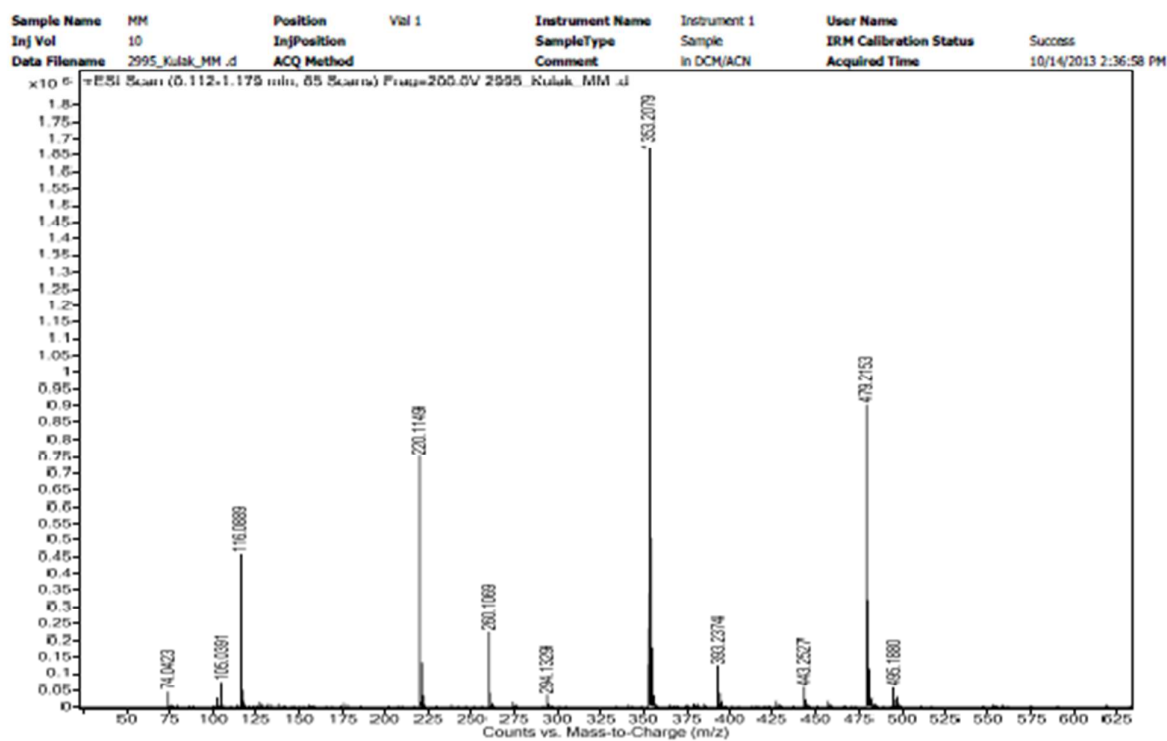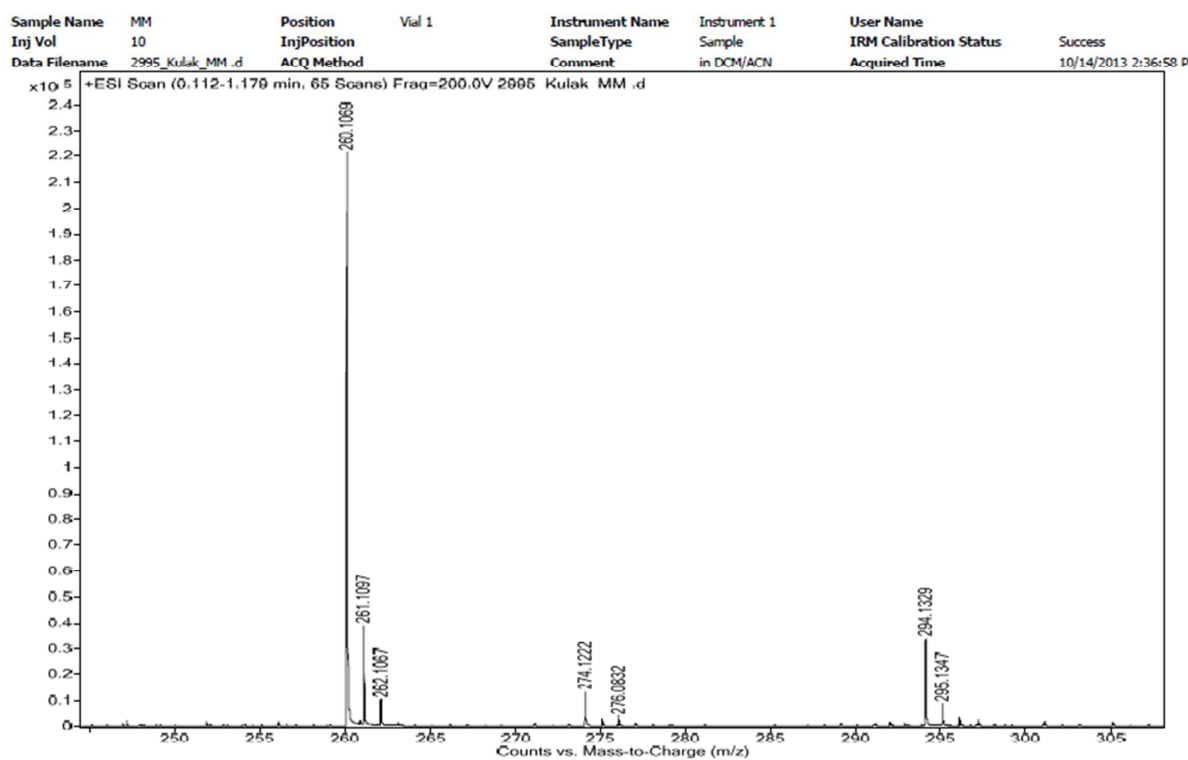

Figure S2. EI-MS of *N*-(3-(methoxydimethylsilyl)propyl)¬benzamide (**2**).

Figure S3. ESI-MS of *N*-(3-(methoxydimethylsilyl)propyl)¬benzamide (**2**) (survey).

Figure S4. ESI-MS of *N*-(3-(methoxydimethylsilyl)propyl)¬benzamide (**2**) (zoomed).

3. TXRF

3.1. Quantification

With Sherman's equation for TXRF, the respective elemental mass deposition was calculated from the obtained count rates.[2] For the effective excitation intensity correction of the incoming radiant power due to the X-ray standing wave field the software package IMD (Version 5) was used.[3]

To determine the count rates of the characteristic fluorescence lines the recorded fluorescence spectra were deconvoluted employing experimentally derived and physically modeled detector response functions of the SDD.[4] In addition to the modeled fluorescence lines the spectrum is fitted with background contributions from resonant Raman scattering and Bremsstrahlung.[5]

Table S1. Quantification results from reference-free TXRF spectroscopy.

Layer	elemental mass deposition			silane areic density
	C	N	O	
	$\times 10^{15}$ [atoms/cm²]			[molecules/nm²]
1	3.9	0.25	6.8	2.5±0.9
2	6.5	0.38	7.4	3.8±1.3
native oxide (SiO$_2$/Si wafer blank)*	3.2	0.0	7.5	

*The native oxide layer has a thickness of 1.7±0.5 nm as calculated from the total oxygen mass deposition of the blank silicon wafer.

The uncertainties associated with the analytical TXRF quantification results are the relative uncertainties of both experimental and atomic fundamental parameters. For more detailed information see Table S2. The overall relative combined standard uncertainty for the quantification is up to 0.30 for nitrogen with the main contributions to the uncertainty budget originating from relevant atomic fundamental parameters such as fluorescence yields, transition probabilities and photoelectric cross sections ranging from 0.1 to 0.3.[6, 7]

Table S2. Uncertainty budget giving the relative uncertainties for the analytical results obtained by reference-free TXRF.[2, 7]

source of uncertainty	Contribution to the relative uncertainty of $\frac{m_i}{area} / 10^{-2}$		
Element	**C**	**N**	**O**
R_i detected count rate	~0.5	~0.7	~0.1
S_0 current of calibrated photo diode to determine the incident radiant power	0.01	0.01	0.01
σ_{diode,E_0} spectral responsivity of the photodiode	1	1	1
ψ_{in} incident angle	0.7	0.7	0.7
Ω_{det} effective solid angle of detection	4	4	4
$I_{W_{surf}}$ relative intensity of the standing wave field on the surface	5	5	5
$\varepsilon_{det.E_i}$ detection efficiency of the detector	1.5	1.5	1.5
τ_{i,E_0} photoelectric cross section of element i	10	10	10
$\mu_{tot,i,E}$ total absorption cross section of element i	10	10	10
Q_i excitation factor including the fluorescence yield, the transitions probability of the fluorescence line and the jump ratio; the rel. uncertainty is dominated by the rel. uncertainty of the fluorescence yield [2]	30	25	20
relative combined standard uncertainty u_c	**34%**	**30%**	**26%**

3.2. Film thickness estimation

Nanolayer thicknesses were estimated from TXRF silane areic density values using equation 1.[8]

$$surface\ density\ (molecules/nm^2) = \frac{t\ (nm) \times \rho\ (g/cm^3) \times N_A (molecules/mol) \times 10^{-21}\ (cm^3 \times nm^{-3})}{M\ (g/mol)} \quad \textbf{eq.(1)}$$

with film thickness (t), silane density (ρ), Avoagdro constant (N_A), and the molar mass (M) of the silane (without hydrolysable OMe group).

4. XPS

4.1. Quantification

Table S3. CasaXPS quantification results of the unmodified Si wafer with native oxide (SiO_2/Si blank) and silane monolayers **1** and **2** obtained from survey spectra using laboratory XPS.

layer	C	N	O	Si
		[atom-%]		
1	24.7	1.9	39.2	34.2
2	30.9	2.6	35.4	31.1
native oxide (SiO_2/Si wafer blank)*	20.6	–	43.0	36.4

 * The native oxide layer has a thickness of 1.7±0.5 nm as calculated from the total oxygen mass deposition of the blank silicon wafer in the TXRF experiment.

Table S4. Uncertainty budget giving the relative uncertainties for the CasaXPS quantification results obtained for nitrogen.

source of uncertainty	relative standard uncertainty [%]
surface concentration	10
peak fitting (component sum curve & background)	20
inelastic mean free path (IMFP)	20
elastic scattering (EAL vs. IMFP)	2
photoionization cross section	10
electron emission angle, θ	5
relative combined standard uncertainty u_c	**32%**

4.2. Examples of high-resolution core-level synchrotron XPS data

Name	Pos.	FWHM	%Area
C-C/C-H	285.00	1.219	70.55
C-Si	284.22	1.219	19.15
C-N	286.29	1.219	6.31
C=O	288.02	1.219	3.99

Name	Pos.	FWHM	%Area
NH-C=O	400.25	1.664	90.10
NH3+/NH2-C=O+	402.24	1.232	9.90

Name	Pos.	FWHM	%Area
SiO2	533.42	1.613	93.23
NH-C=O	531.86	1.613	6.77
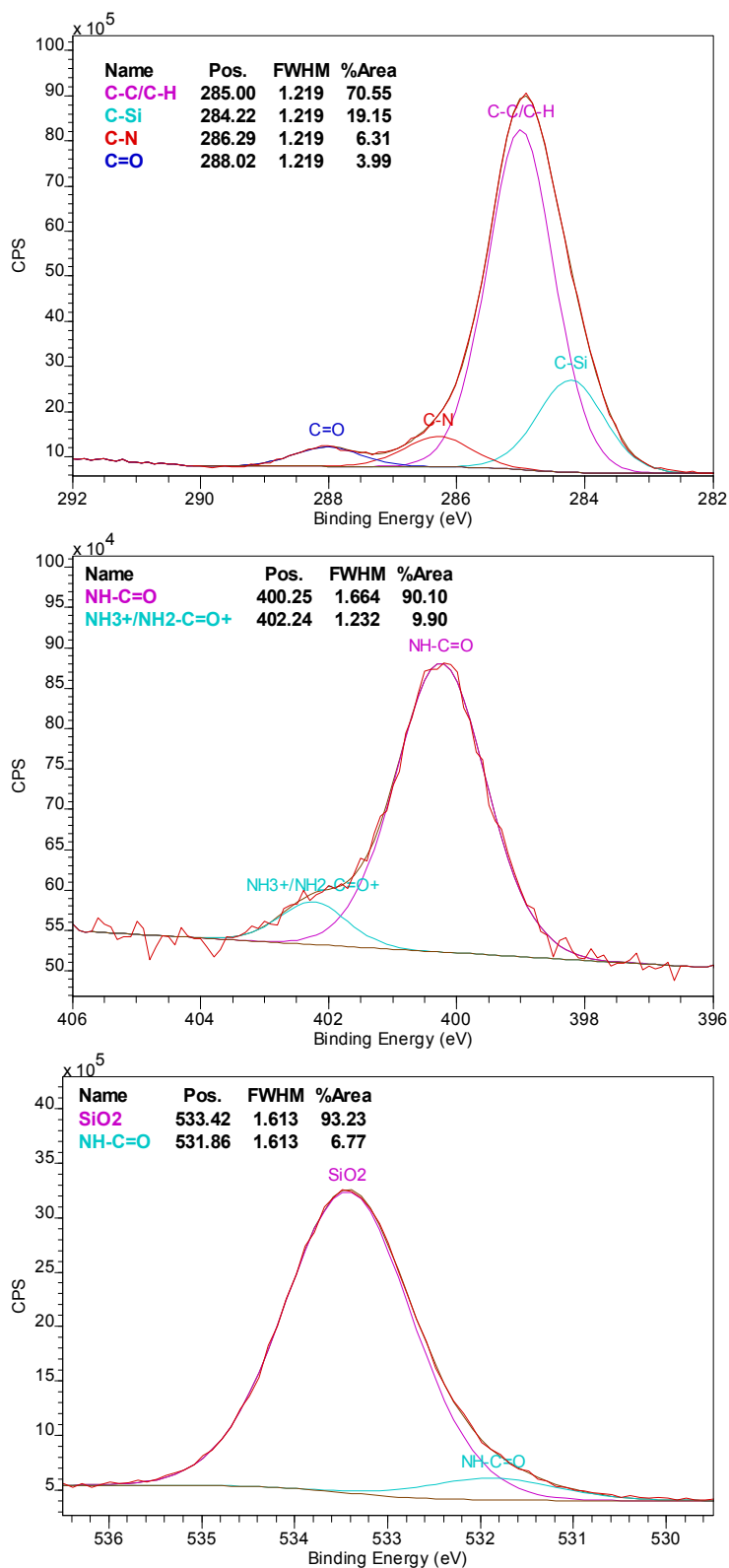
Figure S5. Examples of high-resolution C 1s (top, $h\nu = 385$ eV, $\theta = 60°$), N 1s (middle, $h\nu = 500$ eV, $\theta = 60°$), and O 1s (bottom, $h\nu = 620$ eV, $\theta = 60°$) SR XPS data of amidosilane **2** monolayer acquired at $z_{95} = 1.2$ nm.

Top plot (aminosilane 1):

Name	Pos.	FWHM	%Area
Si(0) 2p3/2	99.01	0.580	31.84
Si(0) 2p1/2	99.56	0.520	15.91
SiO2	103.34	1.550	36.63
Si(-O)1	101.80	1.867	8.79
Si2O	99.96	0.593	5.79
SiO	100.76	0.595	0.70
Si2O3	101.49	0.519	0.32

Bottom plot (amidosilane 2):

Name	Pos.	FWHM	%Area
Si(0) 2p3/2	99.00	0.561	31.56
Si(0) 2p1/2	99.55	0.506	15.77
SiO2	103.29	1.517	36.19
Si(-O)1	101.80	1.701	9.07
Si2O	99.95	0.596	5.95
SiO	100.75	0.590	0.84
Si2O3	101.48	0.741	0.63

Figure S6. Fit of high-resolution Si 2p core-level spectra taken on aminosilane **1** (top) and amidosilane **2** (bottom) layers on silicon oxide surfaces using laboratory XPS ($h\nu = 1486.69$ eV, $\theta = 60°$, $z_{95} \cong 5.7$ nm). The Si 2p peak was fitted according to ref.s [9-12] and include the following Si 2p components: Si^0 (bulk), R_1SiO_3 (silane), SiO_2 (oxide), and silicon suboxide (Si^I_2O, $Si^{II}O$, and $Si^{III}_2O_3$) contributions.

5. Calculation of Si 2p ionization potentials

To interpret experimental data, quantum chemical calculations were carried out to determine 2p ionization potentials for various Si atoms in the tridymite/amidosilan system.

Since we have to deal with a Si-SiO$_2$ interface, with SiO$_2$ being amorphous, it is not straightforward to choose an appropriate model system. In the literature one often uses a silicon bulk model combined with a tridymite structure.[13, 14] For our purpose, it is sufficient to use only the tridymite phase, with an amidosilane molecule on top. Our calculations are based on the crystallographic data published in Ref.[15] to construct a supercell with 532 atoms. We cut the structure along the (0 0 1)-plane with end-standing oxygen atoms on top of the surface. The dimensions of our supercell are 26.17 Å x 29.91 Å x 25.00 Å. Furthermore, all dangling bonds were saturated with hydrogen.

As a result we obtain a surface silanol (OH) group concentration of 4.6 OH groups per nm², which is in perfect agreement with the reported experimental OH concentration of amorphous silica.[16-18] In a first step, we relaxed the top layer. We used the GAPW method as implemented in the CP2K program.[19, 20] As a basis set, we used 6-31G** and a plane wave cutoff of 300 eV. Further, we used density functional theory in the generalized gradient approximation for all calculations. In particular, as an exchange correlation functional, PBE was applied.[21] After optimizing the upper layer, the amidosilane molecule **2** was attached and the upper layer was optimized again with the attached molecule. The resulting tridymite surface model with molecule **2** attached to it is shown in Figure S8. The ionization energies out of various silicon 2p orbitals (I. P.) were calculated by the so-called Δ-KS approach.[22] Here, the ionization energy is the difference between the neutral and core excited system. We used an iglo-III basis for the excitation center to sufficiently account for relaxation effects. The detailed theory is described in Ref. [23].

Four selected Si atoms **Si-1** to **Si-4** were chosen for analysis as indicated in Figure S7. Table S5 shows the calculated ionization energies for these four atoms, out of their 2p orbitals. The lowest ionization energy of the 2p electron is obtained for **Si-1** which is part of the silane molecule **2**. Because all other Si atoms are bound to more than one oxygen atom (as electron withdrawing atom), their ionization energies are shifted to higher values: by 2 eV for **Si-2**, and 2.3 eV for the **Si-3** and **Si-4**. Given the fact that we do not account for different conformers, degrees of substitution or temperature effects, which may lead to further corrections, our results are in principal agreement with the experimental data.

Table S5. Calculated Si 2p ionization potentials (I. P.) for different silicon atoms. The numbers of the silicon atoms **Si-1** to **Si-4** in the table correspond to those in Figure S7b.

atom	I. P. [eV]
Si-1	102.41
Si-2	104.43
Si-3	104.70
Si-4	104.77

a)

b)
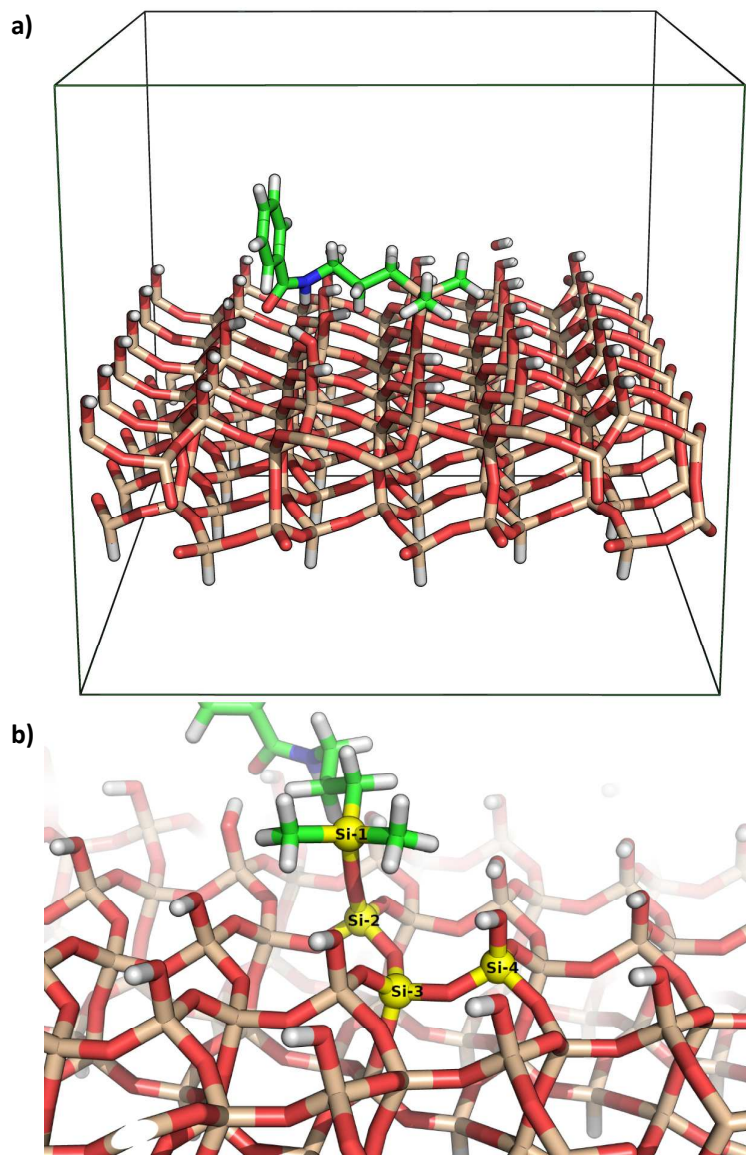
Figure S7. a) The used tridymite surface model with the attached amidosilane molecule **2**. White sticks correspond to hydrogen, beige to silicon, red to oxygen, green to carbon and blue to nitrogen. b) The four investigated silicon atoms **Si-1** to **Si-4** are shown in yellow. The labels **Si-1** to **Si-4** correspond to the Si 2p ionization potentials shown in Table S5.

6. References

1. Poly(silsesquioxane) spherical particle containing ultraviolet light-absorbing group and manufacturing method thereof, 2005, Kim, Y.-B., Saim-Dang Cosmetics Co., LTD., W.I.P. Organization, Korea, WO 2005/105028.
2. Sherman, J., *The theoretical derivation of fluorescent X-ray intensities from mixtures.* Spectrochimica Acta, 1955. **7**(0): p. 283-306.
3. Windt, D.L., *IMD—Software for modeling the optical properties of multilayer films.* Computers in Physics, 1998. **12**(4): p. 360-370.
4. Scholze, F. and M. Procop, *Modelling the response function of energy dispersive X-ray spectrometers with silicon detectors.* X-Ray Spectrometry, 2009. **38**(4): p. 312-321.
5. Müller, M., et al., *Absolute determination of cross sections for resonant Raman scattering on silicon.* Physical Review A, 2006. **74**(1): p. 012702.
6. Beckhoff, B., et al., *Reference-Free Total Reflection X-ray Fluorescence Analysis of Semiconductor Surfaces with Synchrotron Radiation.* Analytical Chemistry, 2007. **79**(20): p. 7873-7882.
7. Zschornack, G., *Handbook of X-Ray Data* 2007: Springer.
8. Bramblett, A.L., et al., *Determination of surface coverage for tetraphenylporphyrin monolayers using ultraviolet visible absorption and x-ray photoelectron spectroscopies.* Surface and Interface Analysis, 2002. **33**(6): p. 506-515.
9. Hollinger, G. and F.J. Himpsel, *Probing the transition layer at the SiO2‐Si interface using core level photoemission.* Applied Physics Letters, 1984. **44**(1): p. 93-95.
10. Himpsel, F.J., et al., *Microscopic structure of the SiO_2/Si interface.* Physical Review B, 1988. **38**(9): p. 6084-6096.
11. Seah, M.P. and S.J. Spencer, *Ultrathin SiO_2 on Si II. Issues in quantification of the oxide thickness.* Surface and Interface Analysis, 2002. **33**(8): p. 640-652.
12. Keister, J.W., et al., *Structure of ultrathin SiO2/Si(111) interfaces studied by photoelectron spectroscopy.* Journal of Vacuum Science & Technology A, 1999. **17**(4): p. 1250-1257.
13. Stevens, M.J., *Thoughts on the Structure of Alkylsilane Monolayers.* Langmuir, 1999. **15**(8): p. 2773-2778.
14. Pasquarello, A., M.S. Hybertsen, and R. Car, *Si 2p Core-Level Shifts at the Si(001)-SiO_2 Interface: A First-Principles Study.* Physical Review Letters, 1995. **74**(6): p. 1024-1027.
15. Graetsch, H., *X-ray powder diffraction study on the modulated high temperature forms of SiO_2 tridymite between 110 and 220 °C.* Physics and Chemistry of Minerals, 2001. **28**(5): p. 313-321.
16. Zhuravlev, L.T., *Concentration of hydroxyl groups on the surface of amorphous silicas.* Langmuir, 1987. **3**(3): p. 316-318.
17. Zhuravlev, L.T., *The surface chemistry of amorphous silica. Zhuravlev model.* Colloids and Surfaces A: Physicochemical and Engineering Aspects, 2000. **173**(1–3): p. 1-38.
18. Rimola, A., et al., *Silica Surface Features and Their Role in the Adsorption of Biomolecules: Computational Modeling and Experiments.* Chemical Reviews, 2013. **113**(6): p. 4216-4313.
19. Lippert, G., J. Hutter, and M. Parrinello, *The Gaussian and augmented-plane-wave density functional method for ab initio molecular dynamics simulations.* Theoretical Chemistry Accounts, 1999. **103**(2): p. 124-140.
20. Hutter, J., et al., *cp2k: atomistic simulations of condensed matter systems.* Wiley Interdisciplinary Reviews: Computational Molecular Science, 2014. **4**(1): p. 15-25.
21. Perdew, J.P., K. Burke, and M. Ernzerhof, *Generalized Gradient Approximation Made Simple.* Physical Review Letters, 1996. **77**(18): p. 3865-3868.
22. Triguero, L., et al., *Separate state vs. transition state Kohn-Sham calculations of X-ray photoelectron binding energies and chemical shifts.* Journal of Electron Spectroscopy and Related Phenomena, 1999. **104**(1–3): p. 195-207.
23. Iannuzzi, M. and J. Hutter, *Inner-shell spectroscopy by the Gaussian and augmented plane wave method.* Physical Chemistry Chemical Physics, 2007. **9**(13): p. 1599-1610.